Cell, Vol. 84, 25–35, January 12, 1996, Copyright ©1996 by Cell Press

Separation of Sister Chromatids in Mitosis Requires the Drosophila *pimples* Product, a Protein Degraded after the Metaphase/Anaphase Transition

Rembert Stratmann and Christian F. Lehner
Friedrich-Miescher-Laboratorium
der Max-Planck-Gesellschaft
Spemannstrasse 37–39
72076 Tübingen
Federal Republic of Germany

Summary

Mutations in the Drosophila genes *pimples* and *three rows* result in a defect of sister chromatid separation during mitosis. As a consequence, cytokinesis is also defective. However, cell cycle progression including the mitotic degradation of cyclins A and B is not blocked by the failure of sister chromatid separation, and as a result, metaphase chromosomes with twice the normal number of chromosome arms still connected in the centromeric region are observed in the following mitosis. *pimples* encodes a novel protein that is rapidly degraded in mitosis. Our observations suggest that Pimples and Three rows act during mitosis to release the cohesion between sister centromeres.

Introduction

The regulation of sister cohesion is of crucial importance for faithful chromosome distribution in mitosis (for reviews see Miyazaki and Orr-Weaver, 1994; Holm, 1994; Holloway, 1995). During prometaphase, sister chromatids have to establish connections to opposite spindle poles. Cohesion keeps the sister chromatids together and thereby facilitates the correct bipolar orientation of sister kinetochores, a two-step process progressing from monopolar to bipolar attachment. In addition to simplifying the task of orienting sister chromatids, cohesion also allows the monitoring of this process. Chromosomes with the correct bipolar orientation are brought under tension by mechanical forces (Nicklas, 1988; McIntosh, 1991) and onto the metaphase plate. Chromosomes that are not attached to both poles are not under tension, and this absence of tension delays the onset of anaphase, as elegantly shown in mantid spermatocytes (Li and Nicklas, 1995).

While cohesion is essential for the orderly formation of the metaphase plate, it must be released to allow the segregation of sister chromatids during anaphase. The final, irreversible release of sister chromatid cohesion occurs rapidly at the metaphase/anaphase transition and simultaneously in all chromosomes. At least in meiosis, the release of cohesion is also controlled differentially in different regions of the chromosome. Cohesion between chromosome arms is lost already at the metaphase/anaphase transition of meiosis I, while cohesion in the centromeric region is lost only at the metaphase/anaphase transition of meiosis II. This sequential loss of cohesion, first from chromosome arms and second within the centromeric region, is essential for the ordered distribution of homologs and sisters in meiosis I and II (Goldstein, 1980; Kerrebrock et al., 1992; Miyazaki and Orr-Weaver, 1992). Differences in the cohesion between chromosome arms and in the centromeric region have also been described in mitotic chromosomes (Cooke et al., 1987; Gonzalez et al., 1991; Sumner, 1991).

The molecular mechanisms that establish and regulate the cohesion between sister chromatids are poorly understood. Proteins with characteristic localizations between sister chromatids, inner centromere proteins (INCENPs) and centromere-linking proteins (CLiPs), have been suggested to promote cohesion (Cooke et al., 1987; Rattner et al., 1988; Earnshaw and Cooke, 1991). In addition, a number of mutations that result in premature chromosome separation are likely to identify gene products involved in cohesion (for references see Miyazaki and Orr-Weaver, 1994).

While the involvement of specific proteins in sister chromatid cohesion remains to be demonstrated, it is clear that replication of topologically fixed DNA results in interlocking of sister chromatid strands. The idea that the final resolution of this interlocking is triggered at the metaphase/anaphase transition constitutes an attractive and simple model for the regulation of sister chromatid cohesion (Murray and Szostak, 1985). A requirement for DNA topoisomerase II activity, which can resolve DNA interlocking, has been clearly demonstrated during mitosis in yeast and in Xenopus extracts (Uemura et al., 1987; Holm et al., 1989; Shamu and Murray, 1992). However, experiments in yeast have also revealed interlocking-independent cohesion between sister chromatids (Koshland and Hartwell, 1987; Guacci et al., 1993, 1994).

In addition to DNA topoisomerase II, the ubiquitin-dependent protein degradation system has been implicated in the release of sister chromatid cohesion at the metaphase/anaphase transition. Inhibitors of ubiquitination prevent anaphase in Xenopus extracts (Holloway et al., 1993). Moreover, the recently identified anaphase-promoting complex, containing *CDC16*, *CDC23*, and *CDC27* in yeast and homologous proteins in other eukaryotes, is not only required for ubiquitin-dependent degradation of B-type cyclins but also for progression beyond metaphase (Tugendreich et al., 1995; Irniger et al., 1995; King et al., 1995). While the degradation of B-type cyclins (the regulatory subunits of the mitosis-promoting cdc2 kinase) is clearly required for exit from mitosis, sister chromatid separation can still proceed in the presence of mutant B-type cyclins that cannot be degraded in mitosis (Holloway et al., 1993; Surana et al., 1993). It appears, therefore, that the ubiquitin-dependent protein degradation system must degrade proteins other than B-type cyclins for progression beyond metaphase. The attractive idea that these unidentified targets, whose degradation is required for progression into anaphase, physically promote the cohesion between sister chromatids remains to be proven.

Here, we describe phenotypic characterizations of the

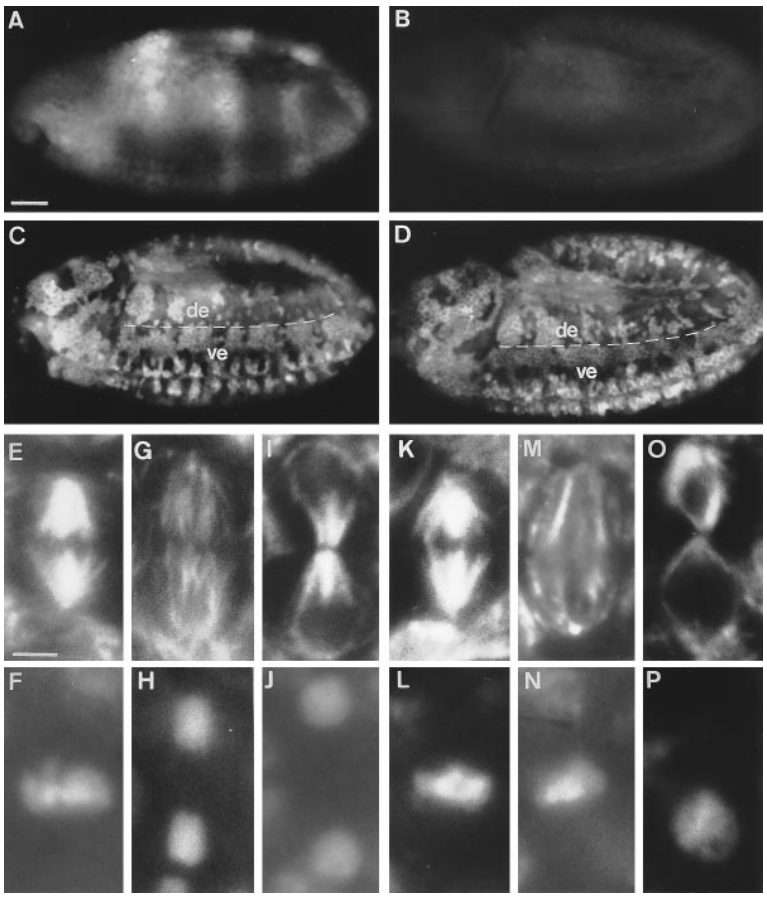

Figure 1. The Defect in Chromosome Distribution Starts during Mitosis 15 in *pim* Mutants

Embryos from heterozygous parents (*pim*^{1}/*CyO*, P[*w*$^{+}$, *ftz–lacZ*]) were aged to the developmental stage during which cells in the ventral epidermis (ve) progress through mitosis 14 and cells in the dorsal epidermis (de) through mitosis 15. Embryos were fixed and labeled with antibodies against β-galactosidase (A and B), allowing the identification of either homozygous *pim*^{1}/*pim*^{1} embryos (B, D, and K–P) or sibling embryos (A, C, and E–J) used as internal controls. Mitotic divisions were visualized by double-labeling with anti–cyclin A antibodies (C and D) or with anti-tubulin antibodies (E, G, I, K, M, and O) and a DNA stain (F, H, J, L, N, and P). The high magnification views show cells at metaphase (E, F, K, and L), anaphase (G, H, M, and N), and telophase (I, J, O, and P). Although cytokinesis is attempted in *pim*^{1}/*pim*^{1} cells, it is abortive and does only very rarely proceed to the extent shown in (O) and (P). Scale bars in (A) and (E) correspond to 50 and 2.5 μm, respectively.

Drosophila *pimples* (*pim*) and *three rows* (*thr*) genes. These genes are specifically required in mitosis for sister chromatid separation in the centromeric region, and interestingly, the *pimples* product, a novel protein, is degraded after the metaphase/anaphase transition concomitant with cyclin B.

Results

Chromosome Distribution in Mitosis Is Defective in *pimples* Mutants

The *three rows* (*thr*) and *pimples* (*pim*) genes were initially identified in a screen for recessive lethal mutations that result in a cuticular pattern defect in Drosophila embryos (Nüsslein-Volhard et al., 1984). Phenotypic and molecular characterizations revealed a primary defect in chromosome distribution during mitosis in *thr* mutants (D'Andrea et al., 1993; Philp et al., 1993). By comparing the *thr* and *pim* mutants, we noted extensive similarities. In both mutants, abnormalities were first seen during the fifteenth round of embryonic mitoses. Progression through the first synchronous, syncytial mitoses (mitosis 1–13) as well as through the first asynchronous mitosis (mitosis 14), which occurs after cellularization in a complex but reproducible temporal and spatial pattern (Foe, 1989), was not affected. These embryonic division patterns can be visualized by whole-mount labeling of embryos with antibodies against either cyclin A or B (Lehner and O'Farrell, 1989, 1990). Both cyclin proteins accumulate during interphase and are rapidly degraded during mitosis. Cells before metaphase, therefore, are intensively labeled with anti-cyclin antibodies; cells after metaphase are no longer labeled. The embryos shown in Figure 1 were fixed and labeled at a stage when some cells in the ventral epidermis are in the process of going through mitosis 14 (see ve in Figures 1C and 1D). At the same stage, cells in the dorsal epidermis are already in the process of going through mitosis 15 (see de in Figures 1C and 1D). DNA double labeling in regions lacking anti-cyclin labeling revealed many late mitotic figures (anaphase, telophase) in wild-type embryos as expected. However, in *pim* mutant embryos, we observed late mitotic figures only in regions progressing through mitosis 14. In regions where cells should have progressed beyond metaphase 15 according to the lack of anti-cyclin labeling, we did not observe normal ana- or telophase figures (data not shown, but see below).

By DNA and anti-tubulin labeling, we analyzed the mitotic defects in *pim* mutants during mitosis 15 in further detail. Metaphase spindles and plates in *pim* mutants were found to be indistinguishable from wild-type controls (compare Figures 1E and 1F with Figures 1K and 1L). In contrast, cells with microtubule organization typical of anaphase and telophase (Figures 1G–1J) were not observed in *pim* mutants. However, cells with abnormal microtubule organization reminiscent of anaphase and telophase were readily detected, but no chromosome segregation was observed in these cells (Figures

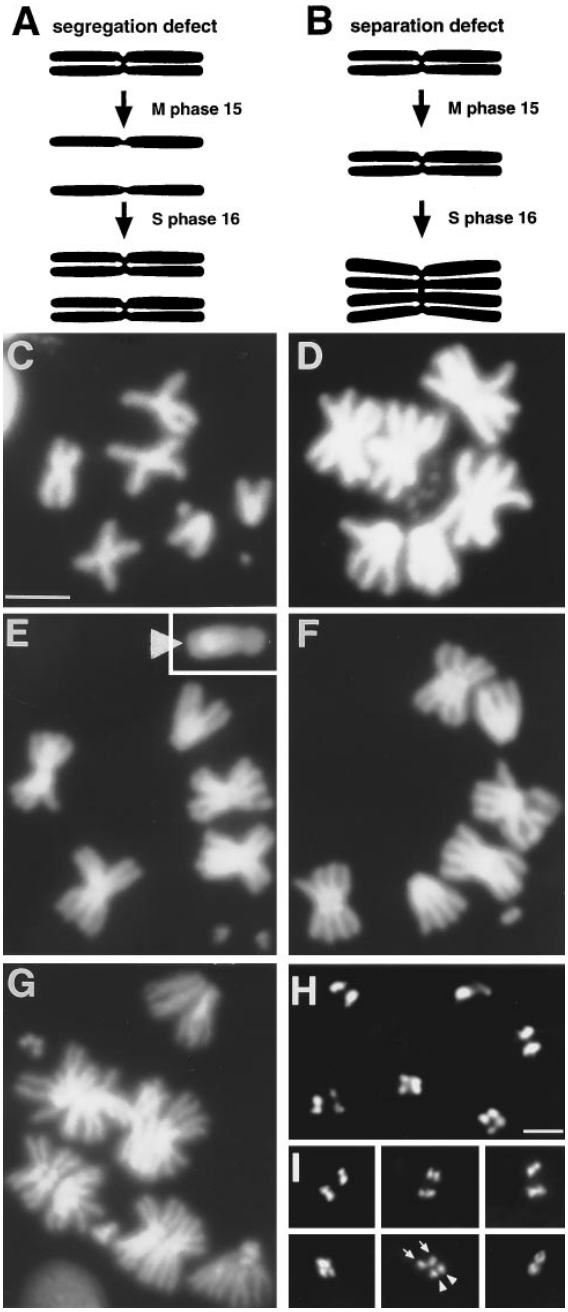

Figure 2. *pim* and *thr* Are Required for Sister Chromatid Separation

(A) If sister chromatids were separated but not segregated to the poles in mitosis 15 in *pim* or *thr* mutants, cells are expected to have twice the number of mitotic chromosomes in mitosis 16.

(B) If sister chromatids were not separated in mitosis 15 in *pim* mutants, cells are expected to have the normal number of chromosomes in mitosis 16. However, these chromosomes should have twice the normal size because of the rereplication during S phase 16.

(C–G) Cytological analyses demonstrate that sister chromatid separation is defective in *pim* and *thr* mutants. Chromosomes present during mitosis 16 are from a female wild-type cell (C), a female pim^{1}/pim^{1} mutant cell (D), a male pim^{1}/pim^{1} mutant cell (E), a female thr^{1B}/thr^{1B} mutant cell (F). The normal number of chromosomes with twice the normal number of arms are present in *pim* and *thr* mutants. The normal number of chromosomes with four times the normal number of arms are present during mitosis 17 in pim^{1}/pim^{1} mutants (G) and thr^{1B}/thr^{1B} mutants (data not shown). In contrast with the other chromosomes, individual arms are not revealed in the Y chromosome (arrowhead in [E]).

(H and I) Whole-mount FISH analysis with a dodeca satellite probe hybridizing to a heterochromatin region very close to the centromere on the right arm of chromosome 3 (Carmena et al., 1993) indicates that centromere proximal regions are replicated in S phase 15 and separated in mitosis 15 in *pim* mutants. Two pairs of closely spaced dots were detected not only in *fzy* mutants (H), in which cells are known to arrest permanently in metaphase before the final separation of sister chromatids (Sigrist et al., 1995), but also in *pim* mutants during mitosis 15 (I). While a field of arrested cells is shown from *fzy* mutants, a selection of six representative cells must be shown from *pim* mutants (I), because cells do not accumulate in a metaphase arrest in *pim* mutants. The two arrows in (I) indicate the pair of dots on one, the arrowheads the pair of dots on the other of the two third chromosomes.

Scale bars in (C) and (H) correspond to 5 μm.

1M–1P). In general, cytokinesis failed because of the central mass of unsegregated chromatin (data not shown). On rare occasions, the generation of anucleate cells apparently occurred (Figures 1O and 1P). These observations indicated that the primary defect in *pim* mutants is a defect in chromosome distribution.

pim and *thr* Are Specifically Required for Sister Chromatid Separation in the Centromeric Region

Chromosomes that are not fully replicated cannot be segregated during mitosis. Checkpoint mechanisms normally prevent entry into mitosis in the presence of unreplicated DNA (Weinert et al., 1994). However, if the *pim* mutation impaired both DNA replication and checkpoint mechanisms, cells might enter mitosis in the presence of unreplicated DNA. To evaluate whether a DNA replication defect is the cause for the chromosome distribution failure in *pim* mutants, we pulse labeled embryos with bromodeoxyuridine (BrdU) (data not shown). During S phase 15, we observed BrdU incorporation in both the early replicating euchromatin as well as in the late replicating heterochromatin, and no differences were observed between *pim* and wild-type embryos. Moreover, BrdU incorporation occurred also during S phase 16 and during later stages in *pim* mutants. These observations suggested that DNA replication is not affected in *pim* mutants. Moreover, they demonstrated that cell cycle progression is not blocked in *pim* mutants despite the failure of chromosome distribution in mitosis 15. The cells in *pim* mutant embryos exit from mitosis 15 and progress through S phase of the next cell cycle (S phase 16).

After S phase 16, cells also enter mitosis 16 in *pim* mutants. This allowed us to distinguish whether *pim* is required already for the separation of sister chromatids or only later in mitosis for the segregation of the separated chromosomes to the poles. If *pim* were defective only in segregation but not in separation of sister chromatids during mitosis 15, cells in *pim* mutants would be expected to have twice the normal number of chromosomes at the stage of mitosis 16 (Figure 2A). Conversely, if *pim* were defective in chromosome separation (and consequently also in segregation), cells would be expected to have the normal number of chromosomes at the stage of mitosis 16; however, these chromosomes would be expected to be twice the normal size in *pim*

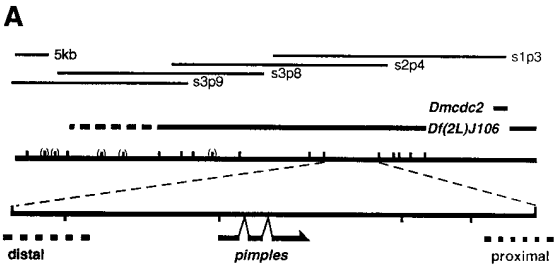

B

```
   5'race       cDNA1
 1 ACTAAGAGTCTCCCATCTCTAGAAAAGTGCCGCTCGTTTTCAGGAATTATTTTAAACTAA

                  cDNA2
61 ACCGCAGCTCACTGCTAGAATTCAATCAAAATACCTTTTTAACACCAATAAATGCTAACA

 1     M  D  Q  I  L  N  K  E  N  T  G  I  N
121 AAATGGATCAGATTTTAAACAAGGAAAACACCGGCATTAATTGTAAGTTGAATTAGGTTC

14                                          L  P  A  N  P
181 GACTCCCGTTCGTGTTAGTAATTACATAGCCATTTATCATTGCAGTGCCAGCGAATCCCA

19 I  K  N  G  V  P  T  N  S  V  L  K  K  P  L  G  N  L  D  N
241 TTAAAAATGGAGTTCCTACAAATTCCGTATTGAAGAAACCTCTTGGTAACCTTGACAATG

39 V  M  H  Q  T  P  G  I  T  P  F  K  S  T  S  L  K  L  E  G
301 TGATGCACCAAACTCCTGGAATAACCCCGTTCAAAAGCACTTCTCTGAAACTCGAGGGTA

59 S  I  A  K  L  S  L  R  K  A  P  K  Q  N  V  V  S  R  D  R
361 GTATTGCCAAGCTTTCGCTGCGAAAGGCCCCCAAACAAAATGTGGTCAGCAGGGATCGCG

79 E  E  V  R  Y  K  T  N  S  C  F  L  G  A  Y  V  L  N  C  E
421 AGGAAGTTAGGTATAAAACAAATAGCTGCTTTTTGGGCGCCTACGTATTGAATTGCGAAT

99 Y  R  V  V  N  L  F  N  Y  T  D  F  P  N  E  K  C  L  K  N
481 ACAGAGTCGTCAATTTGTTCAACTACACTGACTTTCCGAACGAGAAATGTTTGAAGAACT

119 C  S  K
541 GCAGCAAGCGTAAGTACCGCTCATATTAAACAACTCCCCTTGAAAATTGTACTATAAGTT

122                P  V  T  E  T  W  S  E  N  Q  E  G  Y  E  G  L
601 GTATTATTACAGCGGTCACAGAGACCTGGTCGGAAAATCAAGAGGGCTATGAAGGACTAT

138 L  D  Q  L  Y  L  D  L  R  T  L  E  N  N  L  E  N  R  C  L
661 TGGATCAACTTTATCTTGATCTGCGCACATTGGAAAATAATTTGGAAAACAGATGCCTTC

158 P  P  L  D  F  T  D  L  P  Y  I  Y  N  T  E  N  M  E  P  A
721 CGCCCCTAGATTTTACTGACCTGCCATACATATACAACACAGAAAACATGGAGCCTGCAG

178 E  P  E  Y  L  L  N  L  Y  P  P  L  P  N  L  E  G  I  D  V
781 AGCCTGAATACTTATTAAATTTATATCCCCCATTGCCTAACTTGGAAGGCATTGATGTTC

198 L  F  -
841 TATTTTAGATCCTTGTTTAAAAGTTCTATGATTAATTGTAGTTTAATATTTTTTAGCTAG
901 GTATCTTTGTACTACTAATTAATTATTTATTAATGTTATGCTAAGAGAAACTGTTATACC
961 ATTAGCTATCCAAGTTTGTTGTCTCGAATCACATTTGTGAAAAATATTTTTTTTACGCTA
1021 CAATATATTTAGTAGTTTAAGAACCGACATTAAGCCTCCAACAGGCAATTATATGTGTAC
1081 GATGTACCTCGTTTGGAAGTGATTTTGAATTAAAGCAACTATAAAAACT
```

C

allele	mutation	consequence
pim^1	G550 → A	defective splice donor site in intron 2
pim^2	deletion of 514-528	in frame deletion of amino acids 110-114
pim^3	T661 → A	premature stop after amino acid 137
pim^4	619-627 replaced by: ATCAAGA	frame shift after amino acid 123 resulting in addition of 10 unrelated amino acids followed by a stop

Figure 3. Molecular Characterization of the *pim* Gene

(A) A map of the chromosomal walk illustrating the location of *Dmcdc2* and the sequences deleted in *Df(2L)J106* as black lines above the walk. *Dmcdc2* and *Df(2L)J106* were used for the genetic mapping of the *pim* gene. The position of selected cosmids of the chromosomal walk is indicated by the thin lines. The *pim* region defined by RFLP analysis of meiotic recombination events (which is represented enlarged) was found to contain the *pim* gene and parts of a distal and a proximal transcription unit (hatched lines). BamHI sites are indicated in the upper thick line and EcoRI sites in the lower thick line. Additional unmapped sites are indicated in brackets.

(B) DNA sequence and conceptual translation of the transcribed region of the *pim* gene. The sequence starts at the putative transcription start site as revealed by 5′ RACE (Frohman et al., 1988) and ends where the poly(A) tail starts in the cDNAs. The start of the two characterized, independent cDNAs is indicated above the sequence (cDNA1 and cDNA2). 5′ and 3′ untranslated regions as well as the two introns are represented in italics. The poly(A) addition signal is underlined.

(C) Molecular characterization of *pim* alleles. The different *pim* alleles were cloned and sequenced as described in the Experimental Procedures.

mutants because of their rereplication during S phase 16 (Figure 2B).

Analyses of mitotic chromosomes at the stage of mitosis 16 revealed the normal number of chromosomes in *pim* mutants (Figures 2D and 2E). However, compared with wild-type chromosomes (Figure 2C), these chromosomes had twice the normal number of chromosome arms. These arms appeared still connected in the centromeric region. Such "diplochromosomes" were also observed in *thr* mutants (Figure 2F). At later stages, we observed "quadruplechromosomes" in *pim* and *thr* mutants. These chromosomes had four times the normal number of arms connected in the centromeric region (Figure 2G). The abnormal chromosomes were observed with or without preceding colcemid treatment.

To confirm the defect in sister chromatid separation, we performed whole-mount fluorescence in situ hybridization (FISH) with a probe against the dodeca satellite repeat, which is highly enriched in the heterochromatin close to the centromere of the right arm on chromosome III (Carmena et al., 1993). In wild-type mitosis, this probe generates two dots (the maternal and the paternal chromosome III) before sister chromatid separation and four dots after sister chromatid separation (Sigrist et al., 1995). The probe revealed four dots in metaphase plates during mitosis 15 in *pim* (Figure 2I) and *thr* mutants (data not shown). The same characteristic distribution of FISH signals was also observed in the metaphase plates that accumulate in *fizzy* (*fzy*) mutant embryos (Figure 2H). Mutations in *fzy* result in a mitotic metaphase arrest before sister chromatid separation and before cyclin A and B degradation (Dawson et al., 1993, 1995; Sigrist et al., 1995). These FISH experiments indicate that heterochromatic sequences in close proximity of the centromere are replicated and separated in *pim* and *thr* mutants during mitosis 15. Nevertheless, separation of sister chromatids in the centromeric region is not successful during mitosis 15 (and subsequent mitoses) in these mutants. Our cytological analyses demonstrate therefore that *pim* and *thr* are specifically required for the separation of sister chromatids in the centromeric region.

PIM Is a Novel Protein Expressed in Mitotically Proliferating Cells

For a molecular characterization, we mapped *pim* by complementation and meiotic recombination to the region between *Dmcdc2* and the proximal breakpoint of deficiency *Df(2L)J106* (Figure 3A). The corresponding region was cloned by chromosomal walking (Figure 3A).

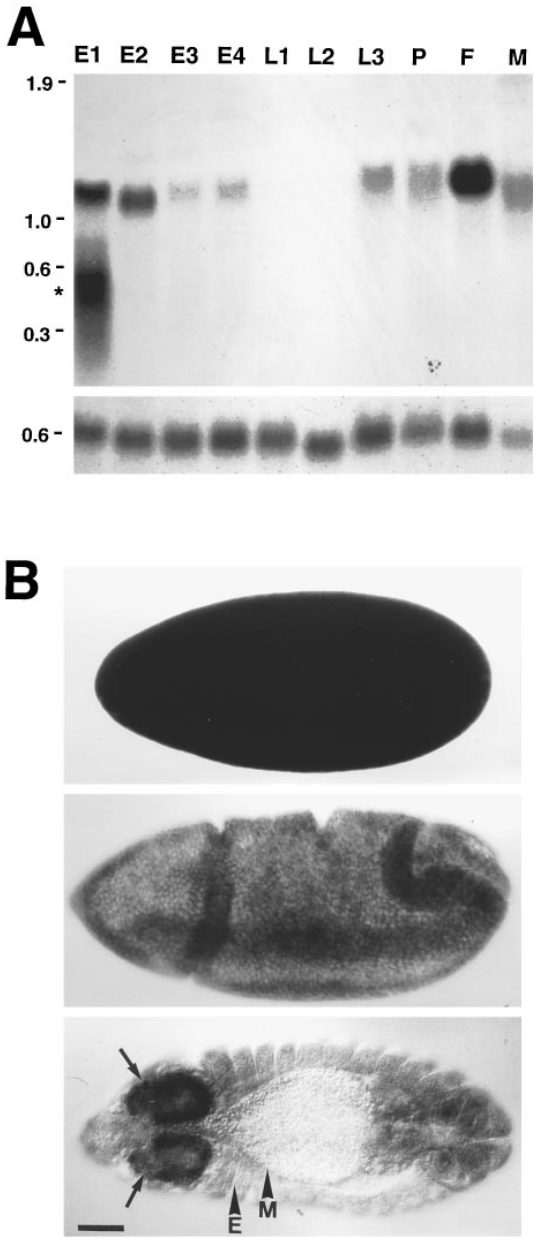

Figure 4. Expression of the *pim* mRNA during Development

(A) Northern blot analysis with a *pim* probe (top) and a probe against the ribosomal protein rp49 (bottom) serving as a loading control. *pim* transcript levels correlate with mitotic proliferation. Each lane contains 5 μg of poly(A)$^+$ RNA from the following developmental stages: 0–2 hr embryos (E1), 2–8 hr embryos (E2), 8–16 hr embryos (E3), 16–22 hr embryos (E4), first larval instar (L1), second larval instar (L2), third larval instar (L3), pupae (P), adult females (F), and adult males (M). The position of molecular weight markers is indicated on the left side. A star indicates a smear detected with the *pim* probe in 0–2 hr embryos. Note that the reprobing of the same Northern blot with the rp49 probe (shown in the bottom panel) excludes artifactual, partial degradation of the corresponding RNA preparation. Since transcription does not normally occur in 0–2 hr embryos, the smear observed with the *pim* probe might indicate specific destabilization of the maternal *pim* mRNA in syncytial embryos.

(B) In situ hybridization with a *pim* probe. High levels of maternal *pim* mRNA are present during the rapid syncytial division cycles (top). After cellularization, *pim* mRNA is found ubiquitously as long as all cells proliferate mitotically (middle) and restricted to the mitotically proliferating nervous system in late embryos (bottom). In the dorsal view of the late embryo, signals are detectable in the brain lobes (arrows) and undetectable in the mitotically quiescent epidermis (arrowhead E) and in the endoreduplicating midgut tissue (arrowhead M). Scale bar corresponds to 50 μm.

Restriction fragment length polymorphism (RFLP) analysis of meiotic recombination events localized the *pim* gene to a fragment containing a single intact transcription unit as indicated by cDNA screening and Northern blotting experiments (data not shown). Transgenes with either a cDNA corresponding to this single intact transcription unit under the control of a heat shock promoter or with a genomic fragment (including 2.3 kb of upstream and 1.3 kb of downstream sequences) rescued the mitotic defect or the lethality, respectively, of *pim* mutants (see below). We conclude therefore that this transcription unit corresponds to the *pim* gene.

Sequencing of genomic and cDNA clones revealed the structure of the transcription unit (Figure 3B). The putative transcriptional start site was determined by 5′-RACE-PCR (Frohman et al., 1988). The conceptual translation of the putative coding sequence results in a sequence that is not related to previously described proteins.

We sequenced the coding region of the original *pim* allele and of three newly isolated alleles. Mutations were found within the *pim* transcription unit in all cases as summarized in Figure 3C.

The expression of *pim* during Drosophila development was analyzed by Northern blotting (Figure 4A) and by in situ hybridization (Figure 4B). These experiments revealed the presence of maternal *pim* transcripts during the early rapid and syncytial cycles 1–13. After cellularization, during the patterned cell division cycles 14–16, *pim* transcripts remained distributed throughout the embryo, but at later embryonic stages, they became restricted to the developing nervous system where mitotic cell proliferation is known to occur. In quiescent or endoreduplicating tissues, we were unable to detect signals above background. *pim* expression therefore appears to be correlated with mitotic proliferation.

The Failure of Chromosome Separation in *pim* Mutants Is Rescued by *pim* Expression Immediately before Mitosis

While our BrdU labeling and FISH experiments argued against an involvement in DNA replication, it remained a possibility that *pim* function is required during S phase, not for DNA replication, but for the assembly of the correct chromatin structure in the centromeric region. The molecular cloning of *pim* allowed the construction of an inducible transgene, and thus, we were able to test whether *pim* function is required during S phase. For this experiment, we constructed a strain carrying mutations in *pim*, cyclin A (*CycA*), and cyclin B (*CycB*) as well as inducible transgenes allowing the expression of *CycA* and *pim* under the control of a heat shock promoter (*Hs-pim; pim^1 Df(2R)59AB/CyO,* P[*w*$^+$, *ftz–lacZ*]; *CycA^5, Hs-cycA/TM3,* P[*w*$^+$, *Ubx–lacZ*]). Embryos

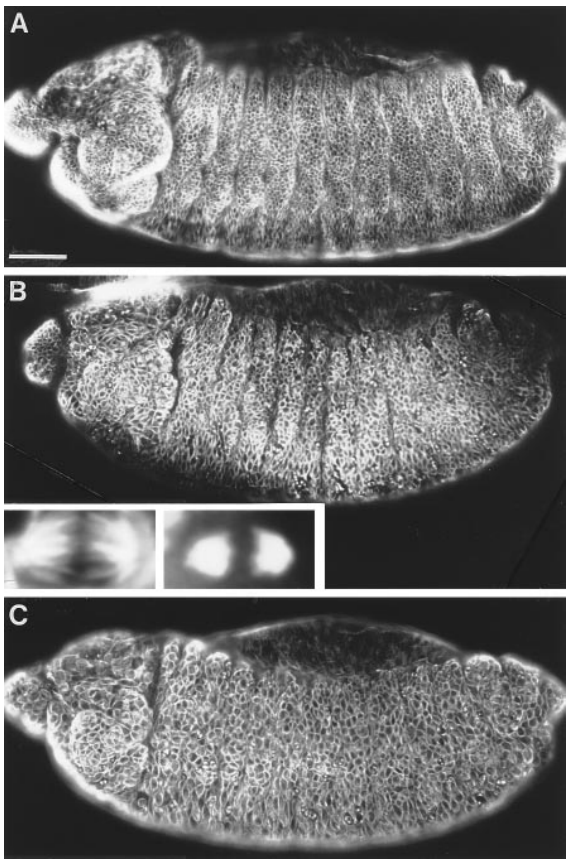

Figure 5. Expression of *pim* Immediately before Mitosis Is Sufficient for Sister Chromatid Separation in Mitosis

Wild-type embryos (A), embryos homozygous for mutations in *pim*, *CycA*, and *CycB* that carried both the heat-inducible transgenes *Hs-pim* and *Hs-cycA* (B), or only *Hs-cycA* (C) were aged to the stage during which the epidermal cells in wild-type embryos are in the G2 phase before mitosis 16. At this stage, embryos lacking both cyclin A and cyclin B are arrested in the G2 phase before mitosis 15 (Knoblich and Lehner, 1993). After incubation at 37°C to express the heat-inducible transgenes (25 min) and recovery at 25°C (3 hr), embryos were fixed and double immunolabeled with anti-tubulin antibodies (A–C) to visualize cell density and with anti-β-galactosidase antibodies (data not shown) to identify the different genotypes (for details see the Experimental Procedures). Whereas the wild-type control (A) displays the normal cell density in the epidermis resulting from completion of both mitosis 15 and 16, *pim*$^-$ *CycA*$^-$ *CycB*$^-$ *Hs-cycA Hs-pim* embryos (B) have a 2-fold lower cell density, and the *pim*$^-$ *CycA*$^-$ *CycB*$^-$ *Hs-cycA* embryos (C) have a 4-fold lower cell density. The increased cell density in the triple mutant embryos with both transgenes (B) compared with the triple mutant embryos lacking the *Hs-pim* transgene (C) indicates that expression of *pim* immediately before mitosis is sufficient to allow a normal mitosis, as also evidenced by the presence of normal anaphase figures (insets in [B]: left, anti-tubulin labeling; right, DNA labeling) observed in triple mutant embryos with both transgenes when fixed after a shorter recovery period (60 min at 25°C). Scale bar in (A) corresponds to 50 μm.

unable to express cyclins A and B zygotically were previously shown to arrest in the G2 phase before mitosis 15 (Knoblich and Lehner, 1993). All preceding mitoses (1–14) occur normally in these double mutants because of maternally contributed stores of the synergistically acting cyclins A and B. However, these stores are no longer sufficient for mitosis 15. Embryos homozygous for mutations in *CycA*, *CycB*, and *pim*, therefore, arrest in the G2 phase before the onset of the mitotic defect caused by the lack of zygotic *pim* expression. With the help of the heat-inducible *Hs-cycA* and *Hs-pim* transgenes, we expressed *CycA* and *pim* in this G2 arrest and analyzed whether expression at this cell cycle stage allows a mitosis including the normal separation of sister chromatids. As illustrated in Figure 5, we found that the heat-induced expression of *CycA* and *pim* allowed progression through an apparently normal division. Completion of a successful mitosis was reflected by epidermal cell densities. At stage 13, when cell proliferation in the epidermis is completed, the cell density as visualized by anti-tubulin labeling is about 4-fold higher in the wild-type epidermis compared with *CycA*, *CycB*, *pim* triple mutants (compare Figures 5A and 5C), because the great majority of wild-type epidermal cells progress through mitosis 15 and 16 instead of arresting before mitosis 15. After heat-induced expression of *CycA* and *pim* in *CycA*, *CycB*, *pim* triple mutants, cell density was roughly doubled (Figure 5B), demonstrating that the expression of *CycA* and *pim* allows one successful cell division. Moreover, when these mutants were analyzed at an earlier stage, soon after the end of the heat treatment, we observed normal anaphase and telophase figures (inset in Figure 5B; data not shown). These observations demonstrate that *pim* function provided late in the G2 phase immediately before mitosis is sufficient for normal sister chromatid separation in mitosis.

PIM Protein Is Rapidly Degraded after the Metaphase/Anaphase Transition

Our polyclonal antibodies raised against bacterially expressed PIM failed to produce a specific signal in immunolabeling experiments with embryos. Similarly, we were unable to detect a PIM protein tagged with a single MYC epitope at the C-terminus and expressed under the control of the *pim* regulatory region. Specific signals were obtained after introducing four copies of a transgene expressing PIM protein C-terminally tagged with six MYC epitopes. The lethality of *pim* mutants was rescued with a single copy of this transgene.

Immunolabeling with the anti-MYC epitope antibodies indicated that the MYC-tagged PIM protein behaved like cyclins A or B (compare Figures 6A and 6B; data not shown). The protein was found to accumulate predominantly in the cytoplasm during interphase 14 (Figure 6A). In prophase and metaphase of mitosis 14, signals were found to be distributed throughout the cell (see m in Figure 6C). In anaphase (see a1 and a2 in Figure 6C), signals were found to decrease, and in telophase, we were unable to detect signals above background (see t in Figure 6C). Gradual accumulation during interphase followed by rapid degradation during mitosis was also observed during the cell cycles of subsequent embryogenesis (data not shown). Although the MYC-tagged PIM protein is degraded in mitosis like cyclins A and B, there is no sequence motif in the putative PIM sequence that fits to the destruction box consensus (RXXLG) that mediates the ubiquitin-dependent mitotic

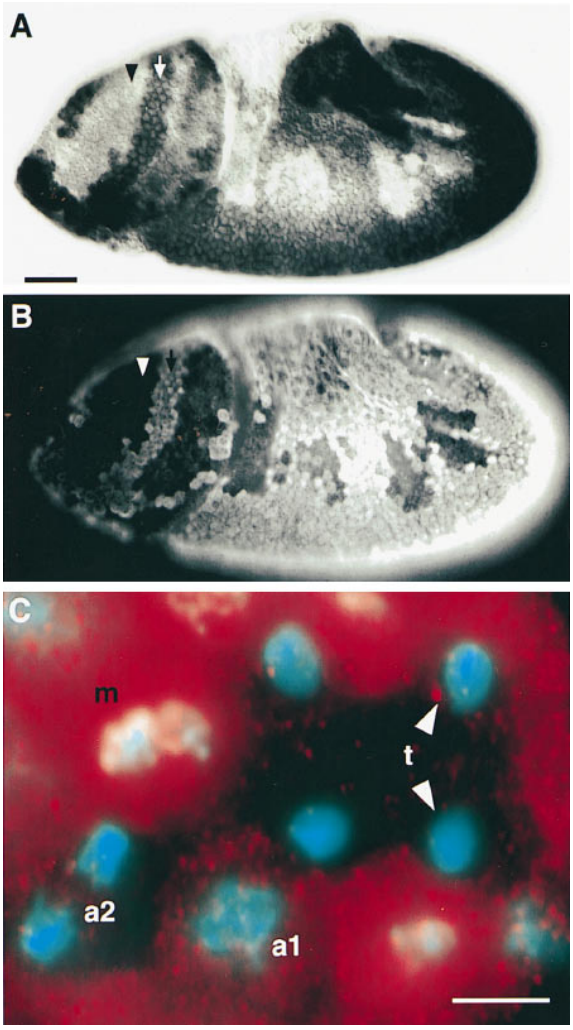

Figure 6. PIM Protein Is Degraded during Mitosis

Embryos with four copies of a transgene allowing the expression of a PIM protein tagged at the C-terminus with six copies of the MYC epitope (Evan et al., 1985) were fixed at the stage of mitosis 14 and double labeled with the anti-MYC antibody (A) and an anti–cyclin A antibody (B). Bound anti-MYC antibodies were visualized by immunocytochemistry resulting in dark signals (A), and bound anti-cyclin A antibodies were visualized by immunofluorescence resulting in light signals (B). Both the MYC-tagged PIM protein and cyclin A are present in cells that have not yet progressed through mitosis 14 (see arrow) and are absent in cells that have already progressed through mitosis 14 (see arrowhead). The high magnification view (C) of immunofluorescent anti-MYC labeling (red) and double labeling with a DNA stain (blue) in cells progressing through mitosis 14 indicates that the MYC-tagged PIM protein, which is present throughout the cell in metaphase (m), is degraded after the metaphase/anaphase transition. Decreasing signal intensity was observed in early (a1) and late anaphase (a2). In telophase (t), signals were no longer above the background levels observed in control embryos that did not express the MYC-tagged PIM protein (data not shown). Scale bars in (A) and (C) corresponds to 50 and 4 μm, respectively.

degradation of these cyclins (Glotzer et al., 1991). The functional significance of a motif in PIM (KKPLGNLDNV, amino acids 30–39) with considerable similarity to the destruction box region in cyclins A and B remains to be tested.

Discussion

The separation of sister chromatids during mitosis must be carefully regulated. While sister chromatid cohesion is required for the bipolar attachment of chromosomes to the mitotic spindle and for chromosome congression into the metaphase plate, the release of cohesion is required for the segregation of sister chromatids to the spindle poles during anaphase. The molecular basis of this regulation is poorly understood, since assays allowing a biochemical analysis have been developed only recently (Shamu and Murray, 1992) and since the powerful genetic analyses in yeast are hampered by the difficulties of cytological analyses. The combination of cytology and genetics in Drosophila has allowed us to identify two genes, *pim* and *thr*, which are specifically required for the release of sister chromatid cohesion during mitosis.

In the absence of *pim* or *thr* function, sister chromatids can no longer be separated in mitosis. The resulting mass of unseparated chromosomes in the equatorial plane of the spindle interferes with a successful cytokinesis that is still attempted in *pim* and *thr* mutants. Except for chromosome distribution and cytokinesis, all other cell cycle steps continue in *pim* and *thr* mutants. The cells reenter interphase and progress through S phase and into the next mitosis despite the previous mitotic defects. Eventually cell cycle progression is stopped by the normal developmental signals in *pim* and *thr* mutant embryos, and the epidermal cells secrete a cuticle, demonstrating that *pim* and *thr* are not required for cell viability. The notion that *pim* and *thr* are only required for mitosis is confirmed by the fact that expression was exclusively detected in mitotically proliferating cells.

Chromosome congression into the metaphase plate is not affected in *pim* and *thr* mutants. Recent experimental evidence indicates that the mechanical forces that are involved in chromosome congression are also involved in chromosome segregation (Rieder and Salmon, 1994; Skibbens et al., 1995). Whether these forces bring about congression or segregation is determined largely by the presence or absence of sister chromatid cohesion, respectively. According to these findings, therefore, the mitotic spindle and the kinetochores are fully functional in *pim* and *thr* mutants, since chromosome congression is observed in these mutants.

Moreover, defects in spindle and kinetochore function are recognized by checkpoint controls in normal mitotic cells. Presumably these defects are recognized by tension-sensitive sensors that signal an absence of tension at kinetochores (Rieder et al., 1994; Li and Nicklas, 1995). The signals generated in response to spindle or kinetochore defects result in a delay in metaphase. For example, colcemid treatment, which interferes with mitotic spindle formation, results in a pronounced metaphase delay in most cell types, and neither sister chromatid separation nor cyclin B degradation occur at the normal time. However, during the first defective mitosis in *pim* and *thr* mutants (mitosis 15), cyclin B appears to be degraded at the normal time, indicating that no spindle or kinetochore defect is recognized in the mutants. This

observation does not necessarily exclude the presence of spindle or kinetochore defects in *pim* and *thr* mutants, because, in principle, these mutants might be defective in the corresponding checkpoint. However, the cells in *pim* and *thr* mutants still arrest in mitosis after colcemid treatment (R. S. and C. F. L., unpublished data), indicating that they are not defective in mitotic checkpoint controls.

The very pronounced metaphase delay that is observed in *pim* and *thr* mutants during mitosis 16 (but not yet during the first defective division, mitosis 15; R. S. and C. F. L., unpublished data) might also result from the presence of a functional checkpoint. During mitosis 16, diplochromosomes resulting from the defect in mitosis 15 are present in the mutants. These diplochromosomes might have four functional sister kinetochores. A bipolar spindle attachment of two of these kinetochores is likely to be sufficient for congression into the metaphase plate. Additional kinetochores that are not engaged in a bipolar attachment might not experience tension resulting in a delay in triggering the metaphase/anaphase transition.

The diplo- and quadruplechromosomes revealed by our cytological analysis indicate that *pim* and *thr* are specifically required for the separation of sister chromatids in the centromeric region. Separation of the chromosome arms apparently still occurred in the mutants. In the case of the Y chromosome, however, no separation of chromosome arms was apparent. This special behavior of the Y chromosome arms is also observed in normal wild-type mitosis (Gatti and Baker, 1989; Gonzalez et al., 1991). The Y chromosome is predominantly composed of heterochromatin. Extensive domains of heterochromatin are also found in the centromeric region of the other chromosomes. Recent analyses of minichromosome transmission in Drosophila have indicated that some of these flanking heterochromatin domains are required for accurate transmission (Murphy and Karpen, 1995). Sister chromatid cohesion, therefore, might be maintained by heterochromatin domains in the centromeric region, which are also found throughout the Y chromosome.

From the phenotypic analyses, the PIM protein might be expected to localize to the centromeric region at least around the metaphase/anaphase transition. Since our immunolocalization required 3-fold overexpression of a MYC-tagged PIM protein, conclusions about subcellular localizations must remain tentative. Interestingly, however, we observed a rapid degradation of this MYC-tagged protein after metaphase. The discrete onset of the PIM phenotype in mitosis 15 strongly argues that the normal nontagged PIM protein is also degraded during mitosis. No phenotype is observed during the early syncytial cycles while maternally derived PIM protein is present. The maternal *pim* transcript is rapidly degraded after mitosis 13 during cellularization (data not shown). The protein translated from the maternal *pim* mRNA before its complete disappearance appears to be sufficient for a normal mitosis 14 in *pim* mutants. After a degradation of this protein in mitosis 14, however, all maternally derived *pim* products (mRNA and protein) appear to be exhausted before mitosis 15 resulting in the tight coupling of phenotypic onset to cell cycle number rather than to age. The same discrete onset of phenotypic defects during mitosis 15 is also observed in *thr* mutants, and preliminary immunfluorescence experiments indicate that the wild-type THR protein is also degraded during mitosis (C. Weise and C. F. L, unpublished data).

The absence of PIM protein early in the cell cycle indicates that *pim* function is required late in the cell cycle. In fact, expressing *pim* immediately before mitosis is sufficient for rescuing the mitotic defects in *pim* mutants. We propose, therefore, that PIM functions at the metaphase/anaphase transition to release the cohesion in the centromeric region. The mitotic degradation might provide one of several levels of regulation preventing a premature separation of sister chromatids during interphase. In the context of the present models for sister chromatid separation (see Introduction), we can speculate that PIM protein might be involved in targeting the anaphase-promoting complex to the centromeric region. The idea that PIM protein is involved in promoting access of DNA topoisomerase II to resolve a final intertwining of sister chromatids at the metaphase/anaphase transition appears unlikely, because centromere separation is still observed in fission yeast DNA topoisomerase II mutants (Funabiki et al., 1993). We note that diplochromosomes were also observed after treating vertebrate cells with various inhibitors like rotenone and okadaic acid (Ghosh and Paweletz, 1992; Matsumoto and Ohta, 1994). A biochemical analysis of PIM and THR function will hopefully clarify the molecular basis of sister chromatid separation in mitosis.

Experimental Procedures

Fly Stocks

Genetic abbreviations are used according to Lindsley and Zimm (1992). The *pim*^{1} (synonym *pim*^{lL}) allele has been isolated by Nüsslein-Volhard et al. (1984). Additional alleles were isolated after X-ray and EMS mutagenesis using standard conditions. Mutations were induced on a *b pr cn wx*^{wxt} *bw* chromosome. One *pim* allele (*pim*^{2}), as well as two large deficiencies deleting *pim*, was obtained from screening 27,000 X-ray mutagenized chromosomes. Two *pim* alleles (*pim*^{3} *and pim*^{4}) were obtained from screening 17,000 EMS-mutagenized chromosomes. The *pim* alleles were balanced with *CyO,* P[*w*$^{+}$, *ftz–lacZ*] for phenotypic analyses. All *pim* alleles appear to result in a complete loss of function. We were unable to detect phenotypic differences in embryos carrying the different *pim* alleles either homozygous or in combination with the deficiency *Df(2L)J27*, and we observed the same early phenotypes with embryos homozygous for this deficiency that includes the *pim* gene. The data shown in the figures were obtained with the allele *pim*^{1}.

The *thr* alleles were isolated by Nüsslein-Volhard et al. (1984), and phenotypic characterizations have been described previously (D'Andrea et al., 1993; Philp et al., 1993). For the cytological analyses described here, we used the apparently amorphic allele *thr*^{lB}. *fzy* alleles and mutant phenotype have also been described previously (Dawson et al., 1993, 1995; Sigrist et al., 1995). The *fzy*^{1} allele was used for the FISH analyses with the dodeca satellite probe.

The deficiency *Df(2R)59AB* deleting the cyclin B gene and the *CycA*^{5} allele as well as the double mutant phenotype has been described by Knoblich and Lehner (1993). The construction of lines with the heat-inducible *Hs-cycA* transgene has also been described previously (Lehner et al., 1991). Lines carrying a *Hs-pim* transgene allowing the heat-inducible expression of *pim* were constructed analogously by inserting a *pim* cDNA into the vector *CaSpeR-hs*

(Pirrotta, 1988) followed by P element–mediated germline transformation. Several independent lines with insertions on different chromosomes were established. Lines carrying transgenes allowing the expression of PIM protein carrying MYC epitope tags (Evan et al., 1985) at the C-terminus were established using constructs in the vector *CasPeR-4* (Pirrotta, 1988).

For the experiment described in Figure 5, we constructed the stock *Hs-pim; pim^1 Df(2R)59AB/CyO,* P[*w*$^+$, *ftz–lacZ*]; *CycA5, Hs-cycA/TM3* P[*w*$^+$, *Ubx–lacZ*] by meiotic recombination and standard genetic crosses. Eggs were collected for 75 min and aged for 14 hr at 18°C. Expression of *Hs-cycA* and *Hs-pim* was induced by floating the egg collection plates for 25 min on a 37°C water bath. Embryos were fixed after either a 1 hr or 3 hr recovery period at 25°C. *Hs-cycA* and *Hs-pim* expression therefore was induced just before the pulse of *string* expression that forces the cells in the dorsal epidermis into mitosis 16 during wild-type development (Edgar et al., 1994). The time of *Hs-cycA* and *Hs-pim* expression was long after completion of S phase 15 that occurs in the dorsal epidermis during development at 25°C between about 3 hr 45 min and 4 hr 45 min. Control experiments involving anti-tubulin and BrdU pulse labeling confirmed the absence of cell divisions in *Hs-pim; pim^1 Df(2R)59AB/ pim^1 Df(2R)59AB; CycA^5, Hs-cycA/CycA^5, Hs-cycA* embryos at the stage during which cells progress through mitosis 15 in wild-type embryos (data not shown).

Cloning

By meiotic recombination using the *pim^1* allele and a chromosome carrying *Sp Dmcdc2^{216A} Tft*, we mapped the *pim* locus 0.03 cM distal from *Dmcdc2*. By screening a cosmid library (NotBamNot–CoSpeR library made by J. W. Tamkun and provided by E. Knust, University of Cologne) with a genomic fragment from the *Dmcdc2* region (Stern et al., 1993), we initiated a chromosomal walk that was terminated after the isolation of a cosmid spanning the distal breakpoint of *Df(2L)J106* that does not complement *pim^1*. The distal breakpoint of this deficiency was localized by Southern blotting and in situ hybridization on polytene chromosomes (data not shown).

After our X-ray mutagenesis had failed to generate breakpoints allowing the identification of the *pim* gene in the 70 kb DNA of the chromosomal walk, we carried out an RFLP analysis of meiotic recombination events to narrow down the location of the *pim* gene. For the isolation of meiotic recombination events, we used *J* and *Dmcdc2* as genetic markers. While *Dmcdc2* is proximal to *pim*, *J* was mapped distal to *pim*. RFLP mapping of various independent recombination events using standard Southern blotting experiments placed the *pim* locus within an 8 kb BamH1 fragment (Figure 3A) (details are provided on request).

Using genomic DNA encompassing the putative *pim* region, we screened a λZAP and a plasmid cDNA library made from ovarian and 0–4 hr RNA, respectively (Hay et al., 1988; Brown and Kafatos, 1988). Two *pim* cDNAs, one isolated from the plasmid library (cDNA1) and one isolated from the λZAP library (cDNA2), were completely sequenced using a Sequenase kit (United States Biochemical). Except for some polymorphisms, both sequences were colinear and contained a single long open reading frame. No stop codon was found in the same frame preceding the putative initiation codon of the *pim* coding sequence in either cDNA2 or cDNA1 that extended for an additional 63 bp in the 5′ region. However, a stop codon was found in the additional 5′ sequence obtained from a fragment isolated by 5′-RACE (Frohman et al., 1988) with a *pim*-specific primer (5′-GGC AGG TCA GTA AAA TCT AGG GGC G-3′) using RNA from embryos and a 5′-RACE kit (GIBCO). Sequence similarities were searched in the EMBL database using FASTA.

The genomic sequence was determined after subcloning cosmid fragments into Bluescript KS(+). For the sequence analysis of the mutant *pim* alleles, we identified homozygous mutant progeny from stocks carrying a *pim* allele over *CyO*, P[*w*$^+$, *ftz–lacZ*] with a PCR method (Knoblich et al., 1994). After identification, we isolated the genomic DNA from homozygous mutant embryos and amplified the *pim* gene enzymatically using the primers 5-AT GGATCC TCA TTA CCA TCG TTT CAG ATG AAC G-3′ (hybridizing just upstream of the putative transcriptional start) and 5′-TA GGATCC GCC TGT TGG AGG CGG AAT GTC GGT TC-3′ (hybridizing in the 3′ untranslated region). These fragments were sequenced after cloning into Bluescript KS(+) using the BamHI sites introduced by the primers. To exclude PCR artifacts, we confirmed the putative mutant sequences in a second clone obtained after an independent PCR reaction. Sequencing revealed the presence of a number of polymorphisms in the *pim* genes in the different genetic backgrounds. Some of these polymorphisms result in amino acid exchanges in the predicted PIM protein (data not shown, available on request).

For construction of the *Hs-pim* transgene, we cloned the EcoRI–NotI fragment from the *pim* cDNA1 into the corresponding sites of *CaSpeR-hs*. The EcoRI site in cDNA1 is 45 bp upstream of the putative initiation codon; the NotI site is in the vector just downstream of the poly(A) tail (Brown and Kafatos, 1988). Details of the trangene constructions allowing the expression of MYC epitope–tagged PIM protein under control of the *pim* regulatory region are available upon request.

Northern Blotting and In Situ Hybridization

Total RNA from embryos, larvae, or adult flies was isolated according to standard procedures followed by purification of poly(A)$^+$ RNA using a Fast Track mRNA isolation kit (Invitrogen). Poly(A)$^+$ RNA (5 μg per lane) was loaded on an agarose gel containing formaldehyde. Northern blotting and hybridization were done according to standard procedures. As a probe, we used *pim* anti-sense RNA transcribed in vitro in the presence of [α-^{32}P]CTP. RNA loading was controlled by reprobing the Northern blot with a probe detecting the ribosmal protein rp49 transcript (O'Connell and Rosbash, 1984).

In situ hybridization to analyze the *pim* transcript distribution in embryos was done as described by Knoblich et al. (1994).

Immunolabeling, FISH, and Cytological Analysis of Mitotic Chromosomes

Embryos were collected, aged, and fixed according to standard procedures. Pulse-labeling with BrdU and immunofluorescent labeling with a monoclonal antibody against BrdU (Becton-Dickinson), β-tubulin (Amersham), cyclin B (Knoblich and Lehner, 1993), or rabbit antibodies against β-galactosidase (Promega), cyclin A (Lehner and O'Farrell, 1989) have been described previously (Lehner et al., 1991; Knoblich and Lehner, 1993).

For immunolabeling the MYC-tagged PIM protein, we fixed dechorionated embryos in 4% formaldehyde in PBS for 20 min. After devitellinization, we incubated the embryos for 30 min in 10% normal goat serum to block nonspecific binding. Incubation with hybridoma supernatant (diluted 1:1 in PBS containing 5% normal goat serum and 0.1% Triton X-100) containing the mouse monoclonal antibody 9E-10 recognizing the MYC epitope (Evan et al., 1985) was done overnight at 4°C. After washing, we incubated the embryos with a rabbit anti-mouse antibody (2.5 μg/ml; Jackson Immunochemicals) for 2 hr at room temperature. After further washing, we incubated the embryos with Cy3-conjugated goat anti-rabbit antibodies (1.4 μg/ml; Jackson Immunochemicals). Secondary and tertiary antibodies were preabsorbed with fixed embryos before incubation. After the final washing, we labeled the embryos with Hoechst 33258 (1 μg/ml) and mounted them in 70% glycerol, 0.5× PBS, O.05 M Tris–HCl [pH 9.5], 0.5 mg/ml phenylene diamine, 10 mg/ml propyl gallate. Alternatively, the anti-MYC antibodies were visualized immunocytochemically with the help of a Vectastain kit. Images were photographed with a Zeiss Axiophot using Technical Pan film (Kodak) or acquired with a cooled CCD camera (Photometrics) and merged using Adobe Photoshop software.

For FISH experiments, we used a dodeca satellite repeat fragment (Abad et al., 1992) following the protocol described by Sigrist et al. (1995). The protocol used for the cytological analyses of mitotic chromosomes in embryos is also described by Sigrist et al. (1995).

Acknowledgments

We thank Gary Karpen for communicating results prior to publication, Carola Weise for help in constructing various transgenic strains, Henning Jacobs for help in some of the genetic screens, Eva Maria Illgen for technical help, Martin Hülskamp, and the members of the laboratory for comments on the manuscript.

Received August 29, 1995; revised November 8, 1995.

References

Abad, J.P., Carmena, M., Baars, S., Saunders, R.D.C., Glover, D.M., Ludena, P., Sentis, C., Tyler-Smith, C., and Villasante, A. (1992). Dodeca satellite: a conserved G+C-rich satellite from the centromeric heterochromatin of *Drosophila melanogaster*. Proc. Natl. Acad. Sci. USA *89*, 4663–4667.

Brown, N.H., and Kafatos, F.C. (1988). Functional cDNA libraries from *Drosophila* embryos. J. Mol. Biol. *203*, 425–437.

Carmena, M., Abad, J.P., Villasante, A., and Gonzalez, C. (1993). The *Drosophila melanogaster* dodeca satellite sequence is closely linked to the centromere and can form connections between sister chromatids during mitosis. J. Cell Sci. *105*, 41–50.

Cooke, C.A., Heck, M.M.S., and Earnshaw, W.C. (1987). The inner centromere protein (INCENP) antigens: movement from inner centromere to midbody during mitosis. J. Cell Biol. *105*, 2053–2067.

D'Andrea, R.J., Stratmann, R., Lehner, C.F., John, U.P., and Saint, R. (1993). The *three rows* gene of *Drosophila melanogaster* encodes a novel protein that is required for chromosome disjunction during mitosis. Mol. Biol. Cell *4*, 1161–1174.

Dawson, I.A., Roth, S., Akam, M., and Artavanis-Tsakonas, S. (1993). Mutations of the *fizzy* locus cause metaphase arrest in *Drosophila melanogaster* embryos. Development *117*, 359–376.

Dawson, I.A., Roth, S., and Artavanis-Tsakonas, S. (1995). The *Drosophila* cell cycle gene *fizzy* is required for normal degradation of cyclins A and B during mitosis and has homology to the *CDC20* gene of *Saccharomyces cerevisiae*. J. Cell Biol. *129*, 725–737.

Earnshaw, W.C., and Cooke, C.A. (1991). Analysis of the distribution of the INCENPs throughout mitosis reveals the existence of a pathway of structural changes in the chromosomes during metaphase and early events in cleavage furrow formation. J. Cell Sci. *98*, 443–461.

Edgar, B.A., Lehman, D.A., and O'Farrell, P.H. (1994). Transcriptional regulation of *string* (*cdc25*): a link between developmental programming and the cell cycle. Development *120*, 3131–3143.

Evan, G.I., Lewis, G.K., Ramsay, G., and Bishop, J.M. (1985). Isolation of monoclonal antibodies specific for human c-myc proto-oncogene product. Mol. Cell. Biol. *5*, 3610–3616.

Foe, V.E. (1989). Mitotic domains reveal early commitment of cells in *Drosophila* embryos. Development *107*, 1–22.

Frohman, M.A., Dush, K., and Martin, G.R. (1988). Rapid production of full length cDNAs from rare transcripts amplification using a single gene-specific oligonucleotide primer. Proc. Natl. Acad. Sci. USA *85*, 8998–9002.

Funabiki, H., Hagan, I., Uzawa, S., and Yanagida, M. (1993). Cell cycle–dependent specific positioning and clustering of centromeres and telomeres in fission yeast. J. Cell Biol. *121*, 961–976.

Gatti, M., and Baker, B.S. (1989). Genes controlling essential cell-cycle functions in *Drosophila melanogaster*. Genes Dev. *3*, 438–453.

Ghosh, S., and Paweletz, N. (1992). Okadaic acid inhibits sister chromatid separation in mammalian cells. Exp. Cell Res. *200*, 215–217.

Glotzer, M., Murray, A.W., and Kirschner, M.W. (1991). Cyclin is degraded by the ubiquitin pathway. Nature *349*, 132–138.

Goldstein, L.S.B. (1980). Mechanism of chromosome orientation revealed by two meiotic mutants in *Drosophila melanogaster*. Chromosoma *78*, 79–111.

Gonzalez, C., Jimenez, J.C., Ripoll, P., and Sunkel, C.E. (1991). The spindle is required for the process of sister chromatid separation in *Drosophila* neuroblasts. Exp. Cell Res. *192*, 10–15.

Guacci, V., Yamamoto, A., Strunnikov, A., Kingsbury, J., Hogan, E., Meluh, P., and Koshland, D. (1993). Structure and function of chromosomes in mitosis of budding yeast. Cold Spring Harbor Symp. Quant. Biol. *58*, 677–685.

Guacci, V., Hogan, E., and Koshland, D. (1994). Chromosome condensation and sister chromatid pairing in budding yeast. J. Cell Biol. *25*, 517–530.

Hay, B., Jan, L.Y., and Jan, Y.N. (1988). A protein component of Drosophila polar granules is encoded by *vasa* and has extensive sequence similarity to ATP-dependent helicases. Cell *55*, 577–587.

Holloway, S.L. (1995). Sister chromatid separation *in vivo* and *in vitro*. Curr. Biol. *5*, 243–248.

Holloway, S.L., Glotzer, M., King, R.W., and Murray, A.W. (1993). Anaphase is initiated by proteolysis rather than by the inactivation of maturation promoting factor. Cell *73*, 1393–1402.

Holm, C. (1994). Coming undone: how to untangle a chromosome. Cell *77*, 955–957.

Holm, C., Stearns, T., and Botstein, D. (1989). DNA topoisomerase II must act at mitosis to prevent nondisjunction and chromosome breakage. Mol. Cell. Biol. *9*, 159–168.

Irniger, S., Piatti, S., Michaelis, C., and Nasmyth, K. (1995). Genes involved in sister chromatid separation are needed for B-type cyclin proteolysis in budding yeast. Cell *81*, 269–278.

Kerrebrock, A.W., Miyazaki, W.Y., Birnby, D., and Orr-Weaver, T.L. (1992). The *Drosophila mei-S322* gene promotes sister chromatid cohesion in meiosis following kinetochore differentiation. Genetics *130*, 827–841.

King, R.W., Peters, J.-M., Tugendreich, S., Rolfe, M., Hieter, P., and Kirschner, M.W. (1995). A 20S complex containing CDC27 and CDC16 catalyzes the mitosis-specific conjugation of ubiquitin to cyclin B. Cell *81*, 279–288.

Knoblich, J.A., and Lehner, C.F. (1993). Synergistic action of *Drosophila* cyclin A and cyclin B during the G2–M transition. EMBO J. *12*, 65–74.

Knoblich, J.A., Sauer, K., Jones, L., Richardson, H., Saint, R., and Lehner, C.F. (1994). Cyclin E controls S phase progression and its down-regulation during Drosophila embryogenesis is required for the arrest of cell proliferation. Cell *77*, 107–120.

Koshland, D., and Hartwell, L.H. (1987). The structure of minichromosome DNA before anaphase in *Saccharomyces cerevisiae*. Science *238*, 1713–1716.

Lehner, C.F., and O'Farrell, P.H. (1989). Expression and function of Drosophila cyclin A during embryonic cell cycle progression. Cell *56*, 957–968.

Lehner, C.F., and O'Farrell, P.H. (1990). The roles of Drosophila cyclin A and cyclin B in mitotic control. Cell *61*, 535–547.

Lehner, C.F., Yakubovich, N., and O'Farrell, P.H. (1991). Exploring the role of *Drosophila* cyclin A in the regulation of S-phase. Cold Spring Harbor Symp. Quant. Biol. *56*, 465–475.

Li, X.T., and Nicklas, R.B. (1995). Mitotic forces control a cell-cycle checkpoint. Nature *373*, 630–632.

Lindsley, D.L., and Zimm, G.G. (1992). The Genome of *Drosophila melanogaster* (San Diego: Academic Press).

Matsumoto, K., and Ohta, T. (1994). Chemical induction of quadruple and octuple chromosomes in Chinese hamster CHO-K1 cells and relationship between their three-dimensional structure and spatial distribution of BrdU-labeled chromatids. Chromosoma *103*, 338–342.

McIntosh, J.R. (1991). Structural and mechanical control of mitotic progression. Cold Spring Harbor Symp. Quant. Biol. *56*, 613–619.

Miyazaki, W.Y., and Orr-Weaver, T.L. (1992). Sister-chromatid misbehavior in *Drosophila ord* mutants. Genetics *132*, 1047–1061.

Miyazaki, W.Y., and Orr-Weaver, T.L. (1994). Sister-chromatid cohesion in mitosis and meiosis. Annu. Rev. Gen. *28*, 167–187.

Murphy, T.D., and Karpen, G.H. (1995). Localization of centromere function in a Drosophila minichromosome. Cell *82*, 599–610.

Murray, A.W., and Szostak, J.W. (1985). Chromosome segregation in mitosis and meiosis. Annu. Rev. Cell Biol. *1*, 289–315.

Nicklas, R.B. (1988). The forces that move chromosomes in mitosis. Annu. Rev. Biophys. Biophys. Chem. *17*, 431–449.

Nüsslein-Volhard, C., Wieschaus, E., and Kluding, H. (1984). Mutations affecting the pattern of the larval cuticle in *Drosophila melanogaster*. I. Zygotic loci on the second chromosome. Roux's Arch. Dev. Biol. *193*, 267–282.

O'Connell, P., and Rosbash, M. (1984). Sequence, structure, and codon preference of the *Drosophila* ribosomal protein 49 gene. Nucl. Acids Res. *12*, 5495–5513.

Philp, A.V., Axton, J.M., Saunders, R.D.C., and Glover, D.M. (1993). Mutations in the *Drosophila melanogaster* gene *three rows* permit aspects of mitosis to continue in the absence of chromatid segregation. J. Cell Sci. *106*, 87–98.

Pirrotta, V. (1988). Vectors for P-element transformation in *Drosophila*. In Vectors: A Survey of Cloning Vectors and Their Uses. R. L. Rodriguez and D. T. Denhardt, eds. (London: Butterworths), pp. 437–456.

Rattner, J.B., Kingwell, B.G., and Fritzler, M.J. (1988). Detection of distinct structural domains within the primary constriction using autoantibodies. Chromosoma *96*, 360–367.

Rieder, C.L., and Salmon, E.D. (1994). Motile kinetochores and polar ejection forces dictate chromosome position on the vertebrate spindle. J. Cell Biol. *124*, 223–233.

Rieder, C.L., Schultz, A., Cole, R., and Sluder, G. (1994). Anaphase onset in vertebrate somatic cells is controlled by a checkpoint that monitors sister kinetochore attachment to the spindle. J. Cell Biol. *127*, 1301–1310.

Shamu, C.E., and Murray, A.W. (1992). Sister chromatid separation in frog egg extracts requires DNA topoisomerase II activity during anaphase. J. Cell Biol. *117*, 921–934.

Sigrist, S., Jacobs, H., Stratmann, R., and Lehner, C.F. (1995). Exit from mitosis is regulated by *Drosophila fizzy* and the sequential destruction of cyclins A, B and B3. EMBO J. *14*, 4827–4838.

Skibbens, R.V., Rieder, C.L., and Salmon, E.D. (1995). Kinetochore motility after severing between sister centromeres using laser microsurgery: evidence that kinetochore directional instability and position is regulated by tension. J. Cell Sci. *108*, 2537–2548.

Stern, B., Ried, G., Clegg, N.J., Grigliatti, T.A., and Lehner, C. F. (1993). Genetic analysis of the *Drosophila cdc2* homolog. Development *117*, 219–232.

Sumner, A.T. (1991). Scanning electron microscopy of mammalian chromosomes from prophase to telophase. Chromosoma *100*, 410–418.

Surana, U., Amon, A., Dowzer, C., McGrew, J., Byers, B., and Nasmyth, K. (1993). Destruction of the CDC28/CLB mitotic kinase is not required for the metaphase to anaphase transition in budding yeast. EMBO J. *12*, 1969–1978.

Tugendreich, S., Tomkiel, J., Earnshaw, W., and Hieter, P. (1995). CDC27Hs colocalizes with CDC16Hs to the centrosome and mitotic spindle and is essential for the metaphase to anaphase transition. Cell *81*, 261–268.

Uemura, T., Ohkura, H., Adachi, Y., Morino, K., Shiozaki, K., and Yanagida, M. (1987). DNA topoisomerase II is required for condensation and separation of mitotic chromosomes in *S. pombe*. Cell *50*, 917–925.

Weinert, T.A., Kiser, G.L., and Hartwell, L.H. (1994). Mitotic checkpoint genes in budding yeast and the dependence of mitosis on DNA replication and repair. Genes Dev. *8*, 652–665.

GenBank Accession Number

The accession number for the *pim* sequence reported in this paper is X93653.